

INTEGRATED USE OF INTERFEROMETRIC SAR DATA AND LEVELLING MEASUREMENTS FOR MONITORING LAND SUBSIDENCE

Yueqin Zhou^{*}, Martien Molenaar^{*}, Deren Li^{**}

^{*}International Institute for Aerospace Survey and Earth Sciences (ITC), the Netherlands

zhouyq@itc.nl, molenaar@itc.nl

^{**} Wuhan Technical University of Surveying and Mapping, China

dli@hp827s.wtusm.edu.cn

KEY WORDS: Land subsidence, Monitoring, Levelling, Differential SAR interferometry, Integration.

ABSTRACT

Land subsidence caused by withdrawal of groundwater has become one of the most serious hazards in many parts of the world, particularly in densely populated and economically developed coastal areas. Levelling is widely applied, as one of the most accurate geodetic techniques, in the world for monitoring land subsidence. But, when levelling is applied over areas of hundreds of square kilometers, the discrete point technique is not effective to represent deformation unless very densely distributed points are measured, which in turn costs a lot of money and time.

Differential SAR interferometry (D-InSAR) is a remote sensing technique that can be used for monitoring small surface movements, such as co-seismic and post-seismic movements, land subsidence, land slide, ice motion etc. However, the quality of D-InSAR products are largely degraded by many factors, which in turn makes the accuracy of D-InSAR is not high enough to measure cm-level subsidence.

An optimal solution to solve the above problems is to integrate D-InSAR with levelling. Using the sparse levelling measurements as ground control and ground truth, the D -InSAR products can be quantitatively assessed; and furthermore, the errors can be modelled. This integrate method has been tested in Tianjin area. The preliminary results show that: (1) D -InSAR can detect the cm-level subsidence in the urban area where the coherence is high enough; (2) the errors between the subsidence values measured by D-InSAR and those by levelling can be quantitatively modelled, and thus the accuracy of D-InSAR products can be improved.

1. INTRODUCTION

With the rapid development of economy, which increases the requirements of fresh water, land subsidence caused by groundwater extraction has become serious hazard in many parts of the world, particularly in densely populated and economically developed coastal areas. Even though this kind of subsidence is often very slow (e.g. a few centimeters per year), it can have serious damage on the infrastructure since it is often large spatial extent, and can be up to several meters after long-term acceleration.

Levelling is widely applied, as one of the most accurate geodetic techniques, in the world for monitoring land subsidence. The applications of the technique may sometimes be limited by cost since it can only provide subsidence information at a spatially discrete set of locations, hence a large amount of point measurements are required in order to cover a large area to obtain the spatial distribution in detail. And also interpolation is needed to get a continuous two -dimensional coverage.

Differential SAR interferometry (D-InSAR) is a new remote sensing technique for monitoring small surface movements, such as co-seismic and post-seismic movements, land subsidence, land slide, ice motion etc. Unlike levelling, the technique provides movement information with continuous, non-interpolated coverage. This characteristic makes it very effective for measuring surface movements over large areas. D-InSAR is effective for measuring co-seismic movements that are sudden events. That has been demonstrated in many applications, among which is the Landers (California) earthquake in 1992 (Massonnet *et al.*, 1993; Zebker *et al.*, 1994). The applications of D-InSAR to measure cm-level subsidence have been investigated (Kooij, 1995a, 1995b, 1997; Massonnet, Holzer and Vadon, 1997). However, there are many factors that degrade the accuracy of the differential interferometric results. It is only possible to use D-InSAR to measure cm-level motion if the errors are effectively corrected. One existing method to correct the errors is to average multiple products, an alternative approach is to use empirical models to model the effects. The use of these two methods may sometimes be limited by data availability.

An optimal solution to solve the above problems is to integrate D-InSAR with levelling. Using the sparsely distributed levelling measurements as the ground truth, the D -InSAR products can be quantitatively assessed; and furthermore, the errors can be modelled. In this paper, we focus on the integrated use of interferometric SAR data and levelling measurements for monitoring slow land subsidence over large areas. The main objective is to improve the accuracy of differential interferometric results by using levelling measurements.

The paper is organized as follows. Section 2 gives a brief description of the differential interferometric SAR. The errors involved in D-InSAR are analyzed in detail, and the model for error modelling in section 3. Some results are presented in section 4.

2. DIFFERENTIAL SAR INTERFEROMETRY

The differential SAR interferometry commonly involves the generation of two interferograms. One interferogram, which comes from two images spanning long time interval, is expected to contain fringes due to both topographic effects and surface movements. The other one, coming either from two SAR images spanning very short time interval, or an external Digital Elevation Model (DEM), contains topographic fringes only. By differencing the two interferograms, the topographic effects are removed from the surface movement fringes, leaving only the effects of surface movements, from which the surface movements can be derived.

Figure 1 shows the geometry for repeat-pass SAR interferometry, in which only one SAR antenna was mounted on the platform. At one time, one SAR image was acquired. A second SAR image was acquired in a repeated pass some time later. Over the time interval between the two passes, a small height change occurred on the ground surface. Now take cell P as an example. Let δh be the small height change occurred at cell P . Assume that the second pass exactly repeated the first, i.e. S_2 coincides with S_1 , then the measured phase difference (interferometric phase) is related to the slant range change due to the height change by:

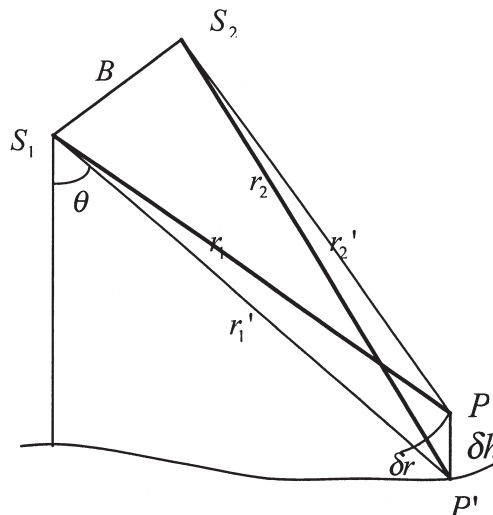


Figure 1. Geometry for repeat-pass InSAR

$$\phi_{2-1} = \frac{4\pi}{\lambda} \delta r = \frac{4\pi}{\lambda} \cdot \delta h \cos \theta \tag{1}$$

Where, λ is the wavelength, θ is the off-nadir angle θ of slant range r_1 . But, if this is not the case, i.e. there is a baseline B between S_1 and S_2 , then the measured phase difference is related to both the topography and the height change:

$$\phi_{2-1} = \frac{4\pi}{\lambda} dr + \frac{4\pi}{\lambda} \delta r = \phi_T + \frac{4\pi}{\lambda} \cdot dh \cdot \cos \theta \tag{2}$$

From (1), the height change dh is derived:

$$dh = \frac{\lambda \cdot (\phi_{2-1} - \phi_T)}{4\pi \cdot \cos \theta} = \frac{\lambda \cdot d\phi}{4\pi \cdot \cos \theta} \tag{3}$$

The topography-related phase ϕ_T can be obtained through using a reference DEM of the same area. The reference DEM can be obtained from two kinds of sources: one is through conventional mapping techniques such as optical stereo-photogrammetry, while the other is through InSAR topographic mapping using a second image pair. In the former case, only two pass images are involved. This is so-called two-pass D-InSAR. In the latter case, the second image pair may be independent of the first pair, or share one image with the first pair, leading to so-called four-pass method and three-pass method, respectively. By means of the reference DEM, the topography-related phase ϕ_T is calculated by:

$$\phi_T = \frac{4\pi}{\lambda} \cdot \frac{B \cos(\theta - \alpha)}{r_1 \sin \theta} \cdot z_p = \frac{4\pi}{\lambda} \cdot \frac{B_{\perp} \cdot z_p}{r_1 \sin \theta} \tag{4}$$

Where, α is the incidence angle of the baseline B with respect to horizontal, B_{\perp} is the perpendicular component of baseline B , z_p is the height of cell P with respect to the reference plane. The resulting interferogram from any of the methods is called the double difference interferogram, which is independent of topography but contains only the small height change (concerning the case of subsidence). The interferometric phase values in the double difference interferogram are still wrapped by 2π . After phase unwrapping, the unwrapped phase values are then converted into the height change using (3). From (3), the height change error is easily derived:

$$\sigma_h = \frac{\lambda}{4\pi \cos \theta} \cdot \sigma_{d\phi} \tag{5}$$

It can be seen from (5) that the accuracy of the height change relies on the accuracy of the differential interferometric phase, which means if the differential interferometric phase values contain errors due to random phase noise and systematic artefacts, the derived height changes contain also errors.

3. ERROR ANALYSIS AND MODELLING

(1) and (2) have been based on the assumption that the interferometric phase is only related to the slant range change due to the topography and the surface motion. In fact, several other factors have the influence on the interferometric phase, either result in noise that degrade the quality of the interferogram, or cause extra phase differences, which are so-called artefacts. The main factors that cause phase noise are radar thermal noise, image misregistration, and temporal decorrelation etc. It has been proven that the radar thermal noise is too small that can be neglected. On the other hand, the image misregistration can be avoided through precise registration up to 1/10 pixel. The most important factor, therefore, is the temporal decorrelation, which is inevitable especially in the case of monitoring very slow land subsidence since in this case a big time interval (on the scale of years) is often required. The phase noise make the phase unwrapping very difficult, which in turn leads errors to the unwrapped phase values.

Among others, the most important factors that may result in the artefacts are the atmospheric effect as well as inaccurate orbital parameters, and inaccurate topographic information used for removing topographic effects. The artefacts due to inaccurate orbital parameters can be corrected if enough accurate ground control points are used. The effect of inaccurate topographic information may be avoided by using the image pair with very small perpendicular baseline, or very accurate reference DEM. The atmospheric effect, therefore, is the major limiting factor for the repeat-pass interferometry (Goldstein, 1995). It can result in up to three extra fringes in the interferogram. These fringes appear to be similar to ground deformation, and hence might be interpreted as the ground deformation.

One way to separate out the atmospheric effect from the true movements is to use multiple observations and average the derived products (Zebker et al., 1997). The other method is to model the atmospheric effects by using the meteorological data at the time of image acquisitions (Hanssen and Feijt, 1996). The use of above two methods is sometimes limited by the data availability.

The approach applied in this paper is to integrate the ground levelling measurements into the differential SAR interferometry. Assume that the overall effects of errors contained in hD-InSAR height change values can be grouped into three parts: blunders, additive random errors, and systematic errors. Under the assumption that land subsidence has a smooth pattern, the blunders are eliminated in the first by low-pass filtering. Then, at a given point, the following equation is assumed:

$$dh = dh' + \bar{d} + u \quad (6)$$

Where dh indicates the true value of height change at the given point, while dh' is denoted as the computed height change from the differential SAR interferometry. The last two terms of (6) are the systematic error and the random noise, respectively. A simple but efficient model to fit the systematic error is polynomial:

$$\bar{d} = a_0 + a_1x + a_2y + a_3xy + a_4x^2 + a_5y^2 + \dots \quad (7)$$

in which, a_0, a_1, \dots are called polynomial coefficients, x, y are the coordinates of the given point. Assuming the random error is the white noise, the polynomial coefficients in (7) can be estimated using the linear regression analysis by means of a certain number of levelling point measurements. Then the height change values are calibrated based on (6) and (7).

4. DATA PROCESSING AND RESULTS

4.1 Test site

Tianjin City, which has experienced the most serious subsidence in China since 1959 due to over exploitation of groundwater, is selected as the test site. The total subsidence area exceeded 13,000 km². Five subsidence centers were identified, marked with cycle in Figure 2. In the urban area, the maximum accumulative subsidence from 1959 to 1986 exceeded 2.5m. The average subsidence rate in 1980-1986 reached to 135mm per year. By adopting water conservation measures in 1986-1988, including closing parts of the wells and refilling water into underground, the rate of subsidence has been significantly reduced down to 20mm/yr. However, the further industrial development has pushed up extraction of groundwater in the suburban area, and the subsidence rate to 50-80mm per year. In order to monitor subsidence, an elaborate network of monitoring sites, shown in Fig.3, has been established since 1986. The levelling survey is carried out once a year in October. Six phase levelling measurements spanning from 1992-1997 were used for the test.



Figure 2. Location of test site and subsidence

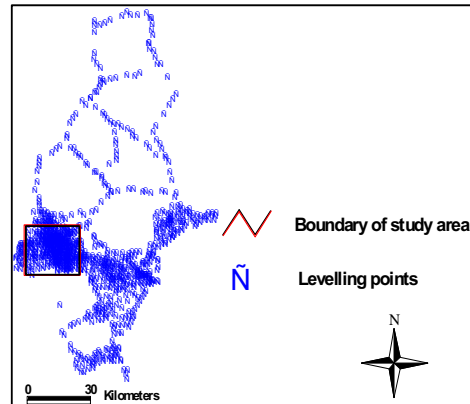


Figure 3. Levelling network

Three scenes of ERS-1/2 SAR SLC data were used in this paper. The relevant information is listed in Table 1.

No.	System	Orbit	Date	Temporal baseline to 23481	Spatial baseline to 23481	
					Para. B_{\parallel}	Perp. B_{\perp}
1	ERS-1	23481	11/01/96			
2	ERS-2	03808	12/01/96	1 day	102	42
3	ERS-2	12826	03/10/97	21 months	-76	-37

Table 1. Spatial and temporal baselines of ERS SAR data

4.2 Levelling data processing

Since the acquisition time of SAR data is different from that of levelling measurements, the temporal interpolation is required to calculate the height values of the levelling points at the time of SAR data acquisitions. Assume the temporal height change at an y point can be modelled by a polynomial:

$$Z_{pi} = Z(t) = b_0 + b_1t + b_2t^2 + b_3t^3 + \dots \quad (8)$$

Where, t denotes the time period with respect to a reference time, $b_0, b_1, b_2, b_3, \dots$ are polynomial coefficients. At the given levelling point, the coefficients are calculated using the linear regression by means of the known levelling measurements. The order of the polynomial is automatically determined through the significance test. Then using the calculated coefficients, the height at the time of SAR scene acquisition is interpolated by (8).

Using the above method, the height values of total 437 levelling points within the study area are calculated for the acquisition time of scene 23481 and 12826. The average RMS value is 0.43 cm, while the standard derivation of RMS value is 0.14 cm. Figure 4 shows the histogram of the RMS at all points. It is, therefore, reasonable to use the polynomial to do temporal modelling.

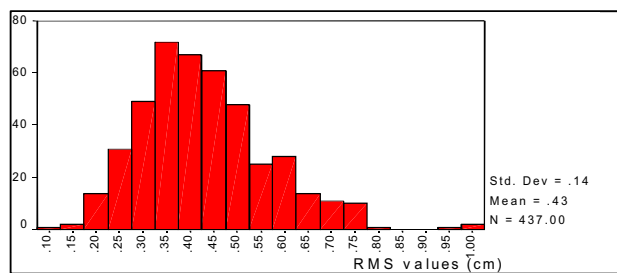


Figure 4. Histogram of RMS of temporal modelling

From the interpolated height values, the height change between the acquisition time of scene 23481 and that of 12826 is calculated at each levelling point, and then the subsidence map is generated, shown in Figure 5.

4.3 InSAR data processing

Atlantis's EarthView InSAR software is used to process the InSAR data. This software provides "DEM mode" to generate DEM, and "Differential mode" with "two -pass", "three -pass", or "four -pass" to make change models. In our experiment, the DEM mode is firstly used to generate the reference DEM from the tandem pair 23481/03808. Then using the reference DEM as "External InSAR DEM", the three -pass differential SAR interferometry is applied to generate the differential interferogram as well as the height change model from the image pair 23481/12826. A subarea with a size of 25km × 23km (seen in Figure 3), which covers the urban and suburban area of Tianjin, is selected for the test. The geocoded differential interferogram and the height change model are illustrated in Figure 6 and Figure 7, respectively.

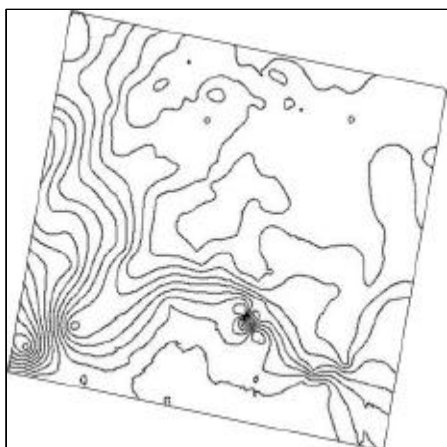


Figure 5. Subsidence map from levelling measurements (96.01-97.10)

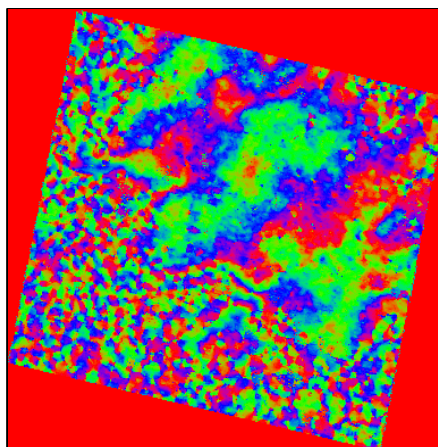


Figure 6. Geocoded D-interferogram

Even though the quality of the differential interferogram is degraded by noise due to low coherence because the time difference between the two passes is too big (21 months), we can still see clear fringes, especially in hard surface areas. Each fringe represents 2.8 cm of slant range change along the line of sight. A similar pattern can be seen by comparison of Figure 5 and Figure 6.

4.4 Error modelling

In order to estimate the errors between the height change measured by D-InSAR and by levelling, the levelling points must be projected into the D-InSAR height change model (Figure 7). This was done using the following method. Firstly, through correlating the geocoded SAR intensity image and the georeferenced orthoimage of the same area, some feature points are identified. Then the coordinate transformation can be done using the coordinates of corresponding points. Finally, the coordinates of the levelling points at the height change model can be calculated through coordinate transformation. The cross marks shown in Figure 7 indicate the levelling points used as the control points for error modelling (total 124 points). Another 226 levelling points are also projected into the height change model, and are used to evaluate the error modelling.

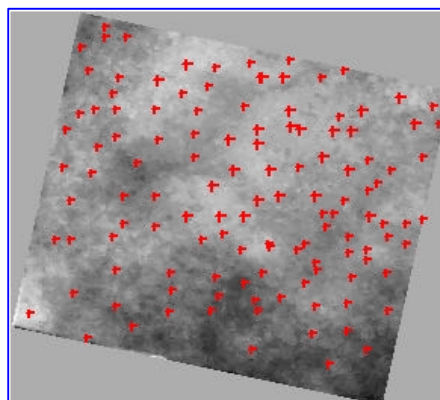


Figure 7. Geocoded height change model

Based on the assumption of (6), the height change differences between the D-InSAR measurements and the levelling measurements contain two parts, i.e. systematic errors modelled by (7), and random errors. With the height change differences at the control points, the coefficients of (7) are estimated by least square method. The coefficients of the polynomial are selected through significance test. Figure 8 gives the histogram of the residuals at the control points. The residuals at the 226 checkpoints are also calculated, leading to the histogram shown in Figure 9.

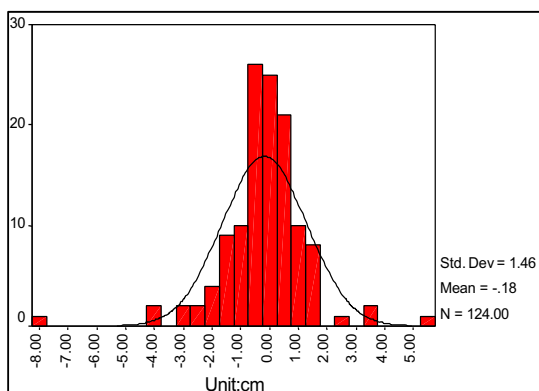


Figure 8. Histogram of residuals at control points

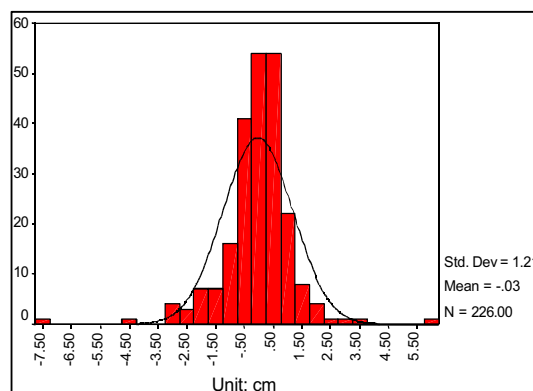


Figure 9. Histogram of residuals at checkpoints

It is obvious that the residuals both at the control points and at the checkpoints follow the normal distribution with zero mean, which means the errors estimated by (7) are the unbiased estimates of the true errors. Therefore it is reasonable to use the polynomial to model errors contained in the D-InSAR products. Using (6) and (7), the D-InSAR height change model is then calibrated.

5. DISCUSSION

In the procedure of error modelling, the levelling measurements are used as the ground truth. In fact, the height values of the levelling points are not original measurements but obtained by interpolation. The interpolation actually decreased the accuracy of control points. In addition, the coordinate transformation can also result in errors. Thus, the standard derivation at the control points and the RMS at the checkpoints with the values of 1.46 cm and 1.21 cm, respectively, do not represent the true accuracy of error modelling but contain extra errors caused in the procedure of error modelling. Therefore, the accuracy of error modelling by the polynomial needs to be further investigated.

6. CONCLUSIONS

The method of integrated use of interferometric SAR data and levelling measurements for monitoring land subsidence was discussed in the paper. The method was tested in Tianjin area. The preliminary results show that: (1) D-InSAR can detect the cm-level subsidence occurred in the urban area where the coherence is high enough; (2) the errors between the subsidence values measured by D-InSAR and those by levelling can be quantitatively modelled, and thereafter, the accuracy of D-InSAR products can be improved. The further work is to design a levelling network containing a limited number points but to be strong enough to control the whole covered area. This will be useful in practical applications to reduce the costs while the accuracy is not decreased.

ACKNOWLEDGEMENTS

The authors would like to knowledge Prof. L.R. Huang, First Land Deformation Monitoring Center, Earthquake Bureau of China, and Mr. Ke Hu, Tianjin Bureau of Surveying and Mapping, for their providing the ground survey data. We would also like to thank Dr.Theo Bouloucos for the helpful discussion and suggestions. This work was supported by "The Science and Technology Development Program (No.9940)" from Tianjin City Constructional Commission, China .

REFERENCES

- Goldstein, R., 1995. Atmospheric limitations to repeat-track radar interferometry. *Geophysical Research Letters*, 22(18): pp.2517-2520.
- Hanssen, R., Feijt, A., 1996. A first quantitative evaluation of atmospheric effects on SAR interferometry. *FRINGE 96*, [http:// www.geo.unizh.ch/rs/FRINGE96/papers](http://www.geo.unizh.ch/rs/FRINGE96/papers) (Sept. 30-Oct.2 1996).
- Kooij, M. W. A. van der et al., 1995a. SAR Land Subsidence Monitoring. BCRS report 95-13, 125pages.
- Kooij, M. W. A. van der et al., 1995b. Satellite radar measurements for land subsidence detection. *Land Subsidence (Proceedings of the Fifth International Symposium on Land Subsidence, The Hague, The Netherlands, 16-20 October 1995)*, Barends, Brouwer & Schröder (eds) © Balkema, Rotterdam, pp.169-177.
- Kooij, M. W. A. van der, 1997. Land Subsidence Measurements at the Belridge Oil Fields from ERS InSAR Data. <http://www.atlsci.com/library/papers/>.
- Massonnet, D. et al., 1993. The displacement field of the Landers earthquake mapped by radar interferometry. *Nature*, 364: pp.138-142.
- Massonnet, D., Holzer, T., and Vadon H., 1997. Land subsidence caused by the East Mesa geothermal field, California, observed using SAR interferometry. *Geographical Research Letters*, 24(8), pp.901-904.
- Shearer, T.R., 1998. A numerical model to calculate land subsidence, applied at Hangu in China. *Engineering Geology*, 49: pp.85-93.
- Zebker, H. A. et al., 1994. On the derivation of coseismic displacement fields using differential radar interferometry: The Landers earthquake. *Journal of Geophysical Research*, October 10, 99(B10): pp.19617-19634.
- Zebker, H.A., Rosen, P.A., and Hensley, S., 1997. Atmospheric effects in interferometric synthetic aperture radar surface deformation and topographic maps. *Journal of Geophysical Research*, 102(B4): pp.7547-7563.